Journal of Biomedical Optics

SPIEDigitalLibrary.org/jbo

Effects of cavitation bubble interaction with temporally separated fs-laser pulses

Nadine Tinne
Gesche Knoop
Nicole Kallweit
Sonja Veith
Sebastian Bleeker
Holger Lubatschowski
Alexander Krüger
Tammo Ripken

SPIE

Effects of cavitation bubble interaction with temporally separated fs-laser pulses

Nadine Tinne,[a,*] Gesche Knoop,[a] Nicole Kallweit,[a] Sonja Veith,[a] Sebastian Bleeker,[a] Holger Lubatschowski,[b] Alexander Krüger,[a] and Tammo Ripken[a]
[a]Laser Zentrum Hannover e.V., Biomedical Optics Department, Hollerithallee 8, Hannover 30419, Germany
[b]Gottfried Wilhelm Leibniz Universität Hannover, Institut für Quantenoptik, Welfengarten 1, Hannover 30167, Germany

Abstract. We present a time-resolved photographic analysis of the pulse-to-pulse interaction. In particular, we studied the influence of the cavitation bubble induced by a fs-pulse on the optical focusing of the consecutive pulse and its cavitation bubble dynamics in dependence on temporal pulse separation in water. As a first result, by decreasing the temporal separation of laser pulses, there is a diminishment of the laser-induced optical breakdown (LIOB) efficiency in terms of energy conversion, caused by disturbed focusing into persisting gas bubbles at the focal volume. A LIOB at the focal spot is finally suppressed by impinging the expanding or collapsing cavitation bubble of the preceding pulse. These results could be additionally confirmed in porcine gelatin solution with various concentrations. Hence, the interaction between the laser and transparent ophthalmic tissue may be accompanied by a raised central laser energy transmission, which could be observed in case of a temporal pulse overlap. In conclusion, our experimental results are of particular importance for the optimization of the prospective ophthalmic surgical process with future generation fs-lasers. [DOI: 10.1117/1.JBO.19.4.048001]

Keywords: fs-laser; laser-induced optical breakdown; laser-induced optical breakdown; photodisruption; cavitation bubble; pulse-to-pulse interaction; high-repetition rate; ophthalmic surgery.

Paper 130877PRR received Dec. 9, 2013; revised manuscript received Mar. 11, 2014; accepted for publication Mar. 13, 2014; published online Apr. 28, 2014.

1 Introduction

The photodisruption as a nonlinear effect of laser-tissue interaction is used in various therapeutic applications of ophthalmic laser surgery. By tightly focusing an ultrashort laser pulse into the transparent tissue, it is possible to manipulate the medium beyond its surface in an arbitrary three-dimensional pattern. Nowadays, there are diverse clinically well-established applications, such as the fs-LASIK (laser *in situ* keratomileusis)[1–5] and keratoplasty,[6] and other intracorneal applications[7] as well as the assistance for cataract surgery.[8] Additionally, fs-laser systems for the reversal of presbyopia[9] are under investigation. In the beginning, clinical fs-laser systems with relatively high pulse energy (>1 μJ) and comparably low-repetition rate (kHz regime) were used in these procedures.[10] A steady decrease in the pulse energies of clinical laser systems,[10,11] along with achievable higher repetition rates, has especially resulted in a significant enhancement in accuracy while simultaneously retaining treatment duration. Therefore, the pulse overlap and interaction between the effects of consecutive laser pulses, and especially the associated cavitation bubbles generated due to the laser-induced optical breakdown (LIOB), have become very important in medical laser applications.

The interaction between a single ultrashort laser pulse and biological tissue has been studied extensively and can be found explicitly described in other publications, for example in Refs. 12–20. Briefly, the photodisruption process can be described as follows: by tightly focusing an ultrashort laser pulse into an aqueous medium like biological tissue, nonlinear absorption processes, such as multiphoton, tunnel, and cascade ionization, are initiated within the focal volume due to the very high intensities.[12,16,21] These lead to the generation of dense free-electron plasma scaling with the amount of energy deposited. If the critical electron density, on the order of $\rho_{cr} = 10^{21}$ cm^{-3}, is exceeded, a LIOB will occur.[12] Afterward, the energy which is deposited in the electronic system is transferred to the atomic system by recombination with parent ions and collision effects. Hence, there is a very fast increase of temperature as well as pressure which leads to a rapid plasma expansion and adiabatic cooling. The buildup of pressure results in a shock wave propagating into the surrounding medium. Its tensile stress component causes the formation of a cavitation bubble by crossing the spinodal limit at temperatures far below the critical point of water.[12,22] In turn, the cavity causes the tissue around the focal volume to rupture. For pulse energies well above the breakdown threshold, the cavity might undergo a series of oscillations before ending in a small persistent gas bubble after some microseconds; amongst others, the maximum bubble radius and the bubble lifetime depend on the laser pulse energy.[12,21] Therefore, this mechanism of cutting tissue via a LIOB is called photodisruption.

Using low repetition rates in the range of some tens of kHz and a temporal pulse separation of some ten microseconds combined with pulse energies close to the breakdown threshold, a laser pulse can hardly interact even with the final stage of effects generated by the previous pulse. However, with higher repetition rates, it is possible that the cavitation bubble of the preceding pulse still exists when the next one is focused nearby; even if the applied laser pulse energy is close to the breakdown threshold. Assuming a bubble oscillation time of 3 μs for pulse

*Address all correspondence to: Nadine Tinne, E-mail: n.tinne@lzh.de

energies scarcely above the breakdown threshold, repetition rates of about 300 kHz and higher would result in a temporal overlap of the subsequent pulse with the previous one's cavitation bubble. Therefore, especially the interaction of different stages of the photodisruption process with a subsequent temporally separated laser pulse becomes more and more important. This interaction between fs-laser pulses and cavitation bubbles may affect the LIOB process of the following laser pulse and hence tissue structures in the vicinity of the laser focus: refraction and defocusing of the laser beam at the oscillating cavity surface, a change of nonlinear absorption efficiency and thus conversion efficiency as well as energy transmission or light scattering at the persistent gas bubbles.

A constitutional similar study was published by Jungnickel and Vogel in 1992.[23] The authors analyzed the interaction efficiency of bursts of up to three subsequent ns-pulses within physiological saline as sample medium amongst others. Plasma formation was used as breakdown criterion via detection of plasma luminescence. As a result, they could observe plasma generation due to the first laser pulse in all cases, whereas plasma formation of subsequent laser pulses was hindered due to the increased breakdown threshold inside the cavity.[23]

The focus of the experiments presented here lies on the characterization and understanding of the fundamental interaction of a cavitation bubble with a subsequently focused laser pulse. This is of great interest for investigation of collateral damage effects and the prospective optimization of the surgical process with high-repetition rate fs-lasers. The cavitation bubble dynamics and the interaction mechanisms were examined by time-resolved photography, which is a well-established method to investigate this effect of laser-material interaction.[12,14,21,24,25] In the present study, two parameters were varied: first, the laser repetition rate and hence the temporal distance of the laser pulses, and second, the applied pulse energy. The bubble-pulse interaction features two clearly separable interaction scenarios with dependence on the investigated parameters.

The experiments presented here reflect not strictly the conditions found in a surgical laser-scanning process, where pulses are applied with the same pulse energy but spatially separated. However, the results shown here comprehend the fundamental case of focusing a subsequent laser pulse into an existing cavitation or gas bubble. This scenario is expected to be achievable with a scanning laser focus. Therefore, the results of our study are discussed especially with respect to collateral damage of surrounding tissue, e.g., the nontransparent retina, in laser surgery, and cavitation bubble overlap-mediated decrease in efficiency during tissue cutting.

2 Materials and Methods

The experimental setup is an installation for time-resolved photography of cavitation bubble dynamics. The system can be divided in two light paths: one is the path of the fs-laser beam, the other for illumination as well as imaging of the cavitation bubbles; both of them are shown schematically in Fig. 1.

2.1 *Time-Resolved Photography*

Time-resolved photography allows for the analysis of fast dynamic phenomena by sectioning the process in specific events. The observation of the oscillating cavitation bubbles with a lifetime of some microseconds is realized by stroboscopic illumination with a flash lamp (High-Speed Photo Systeme, Wedel, Germany) with a flash duration of 17.43 ± 0.55 ns

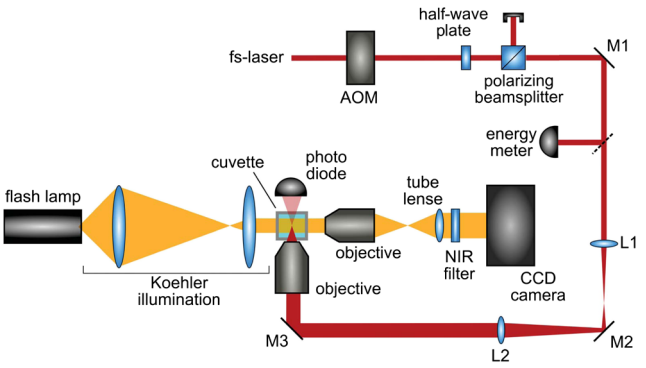

Fig. 1 Schematic depiction of the experimental setup of the laser system (red) and the illumination path (orange). Single pulses of the fs-laser are selected by an acousto-optic modulator (AOM), half-wave plate, and polarizing beam-splitter cube allow for laser power adjustment. The focal region inside the water-filled cuvette is illuminated homogeneously by Koehler illumination and a magnified image of the cavitation bubble is reproduced on the chip of the CCD camera.

(full width at half maximum). In the experimental setup, the illumination path is arranged perpendicular to the direction of laser focusing (see Fig. 1). The plane of the optical breakdown is illuminated homogeneously by Koehler illumination,[26,27] which is also used for bright-field microscopes. The observation path consists of an immersion-free long-distance microscope objective (20x, NA = 0.28, Mitutoyo, Kawasaki, Japan), arranged perpendicular confocally with the laser focusing objective, and an adjusted tube lens. This configuration provides a magnified and sharp image on the charge-coupled device (CCD) chip of the camera (Lumenera, Ottawa, Canada).[28]

The controlling and timing are realized by a delay generator (Bergmann Messgeräte Entwicklung KG, Murnau, Germany) with a specified jitter ≤50 ns. By changing the delay of the flash lamp spark as well as the camera CCD chip opening in respect to the applied laser pulse, images at different stages during the bubble oscillation are taken. The dynamics of expanding and collapsing cavitation bubbles can be reconstructed and illustrated by lining up single frames of different bubbles at subsequent delays.[28]

Image analysis of the individual images was done by the open source software *ImageJ*. The procedure included an identification of the bubble contour and fitting of an ellipse to this contour to consider the different axial as well as radial bubble diameter. The value for the bubble radii was calculated by taking into account the system's magnification of about 19 (equivalent object sampling size of 1 pixel = 0.34 μm, CCD chip pixel width of 6.45 μm), which was determined by traversing a needle within the Koehler-illuminated plane using a micrometer stage.

2.2 *Focusing of Temporally Separated fs-Laser Pulses and Cavitation Bubble Generation*

The second light path, also shown in Fig. 1, is used for laser power adjustment, beam expansion between the laser system and the point of LIOB, and especially for realizing different scenarios of temporal pulse overlap. The following analysis of the temporal pulse-to-pulse interaction was performed with two different fs-laser systems: (1) "μJewel" by IMRA America Inc. (Ann Abor, USA) with central wavelength $\lambda = 1040$ nm; pulse width $\tau = 389$ fs; repetition rate $f_{rep} = 100$ kHz and (2) "Cazadero" by Calmar Laser Inc. (Sunnyvale, USA) with

central wavelength $\lambda = 1030$ nm; pulse width $\tau = 330$ fs; repetition rate $f_{rep} = 120$–1000 kHz.

For external triggered pulse picking, the laser beam is coupled into an acousto-optic modulator (AOM). The laser beam is focused into a sample medium filled cuvette by a second immersion-free high numerical aperture (NA) microscope objective (NA = 0.65, Olympus, Hamburg, Germany) after adapting the beam diameter by a lens telescope. Here, it has to be noticed that the measurements with the "μJewel" laser system were performed with a water-immersion microscope objective of NA = 0.5; the details of this previous setup can be found in Ref. 28, 29. In more solid sample media, that means beside water, a remaining mechanical damage can be induced at the focal spot. Therefore, the cuvette is mounted on a micrometer 3-D stage, which is moved relatively to the focus after every laser pulse application and picture for time-resolved photography.

First, water is used as a model substance for the transparent tissue of the crystalline lens or the cornea. As was shown in Refs. 12, 14, 21, 24, and 25 for corneal tissue, the optical and thermodynamic features of water also determine the LIOB process and cavitation bubble occurrence in these highly hydrated tissues. Furthermore, porcine gelatin (Sigma Aldrich Chemie GmbH, Taufkirchen, Germany) of different concentration (1%, 2%, and 5%) and consistency is utilized as an aqueous sample medium for biological tissue.

2.3 *Experimental Procedure*

Basically, when examining the interaction of two temporally separated laser pulses, three different scenarios are conceivable: (1) application of the second pulse after the cavitation bubble collapse generated by the first pulse, i.e., focusing in the existing remaining gas bubbles, (2) focusing a second laser pulse into an existing cavitation bubble, and (3) application of two successive pulses to the focal spot before the rise of a cavitation bubble due to the first pulse. The latter one can only be generated and analyzed using very high-repetition rates of about 10 MHz and more. For this reason, scenario (3) will not be considered in the following.

For the repetition rate of the "μJewel" laser system is restricted at 100 kHz, different temporal pulse overlap scenarios were realized by variation of the parameter of pulse energy. With increasing laser pulse energy, the maximum cavitation bubble radius R_{max} as well as its lifetime T_c increase: $R_{max} \sim T_c$ and $R_{max} \sim E_{cav}^{(1/3)}$.[12] Particularly, the cavitation bubble energy E_{cav} depends on the deposited laser pulse energy, while the efficiency of applied energy converted into deposited energy strongly depends on the laser pulse duration as well as wavelength.[30] In order to find the particular relation between incident energy and bubble radius, the single bubble dynamics were investigated for different pulse energies at first. Using this relation, the scaling of the pulse energy could be used to control the bubble life time. This way, despite of the limited temporal pulse separation Δt a crucial condition of the well-defined scenarios was determined. At this point, it is recommended for an optimum comparability of the following results to define a dimensionless overlap parameter, i.e., the ratio of pulse separation $\Delta t = 1/f_{rep}$ to cavitation bubble lifetime T_c:

$$\eta_t = \Delta t / T_c. \quad (1)$$

This overlap parameter will be used as a retrospective parameter for an optimum supplementary comparison of the following results and the description of the basic interaction scenarios in water, although its prospective usage in a surgical laser control would require free choice of repetition rate and pulse energy and a knowledge of LIOB threshold energy and rheology of the tissue. Corresponding to the overlap scenarios mentioned above, these comply with the overlap parameter as follows: (1) $\eta_t > 1$ and (2) $\eta_t < 1$. For the "μJewel" laser system and hence a constant repetition rate of 100 kHz, it has been found that the scenarios (1) and (2) can be achieved when operating at laser pulse energies of 6-times (focusing the following pulse into the persistent gas bubbles) and 12-times breakdown threshold (focusing the subsequent pulse into an existing cavity), respectively. To confirm those first results of two directly succeeding laser pulses [measurement (i)], the following measurements were also performed (each with the pulse energies mentioned above): (ii) applying two laser pulses with a double pulse interval of $\Delta t = 20$ μs, and (iii) focusing three consecutive pulses of $\Delta t = 10$ μs each separation (similar to Ref. 23). Afterwards, each sequence of cavitation bubble oscillation was analyzed by evaluating the bubble radius at a particular time. Additionally, measurement (iii) was complemented by an analysis of the transmitted pulse energy using a fast photodiode behind the laser focus. The detector measured the pulse energy content of a central part of the transmitted beam profile. Neglecting scattering effects or beam refraction, this signal was assumed to be proportional to the energy of the entire transmitted beam in all cases. Hence, the results of the transmission measurement are not absolute but relative values and in the case of absorption represent an approximation to the lower limit of the absolute transmission values.

Furthermore, similar measurements were performed with the "Cazadero" laser system. In addition to the measurements (i) to (iii) mentioned above, the repetition rate was varied from 120 to 1000 kHz to analyze its influence on the interaction within the two scenarios (1) and (2). Again, two or more laser pulses were focused at the same focal spot, which was observed via time-resolved photography, and the central laser power transmission was measured with a photodiode.

3 Results and Discussion

3.1 *Determination of the Laser-Induced Optical Breakdown Threshold and Single Cavitation Bubble Dynamics*

To compare and evaluate the following measurements, the threshold above which a LIOB occurs was first determined. In the fs-regime, the most reliable criterion to determine the breakdown threshold is the detection of a cavitation bubble.[12,18,30] At the breakdown threshold, the cavitation bubble radius is well below 1 μm,[30] which is below the optical resolution of 2.32 μm (minimum separability) of the microscope. A more exact measurement of LIOB threshold would be to measure the onset of scattered light by the cavitation instead of its shadow.[30,31] Because the precise determination of threshold energy was not the main scope of this study, the respective energy value was taken as breakdown threshold at which a cavitation bubble in >90% of the shadow images is detectable. Hence, the threshold measurement is an upper limit approximation of the LIOB threshold value. After estimating and deducting the energy losses within the experimental setup (by measuring the laser energy within the following course of the laser beam up to the incoming aperture of the microscope

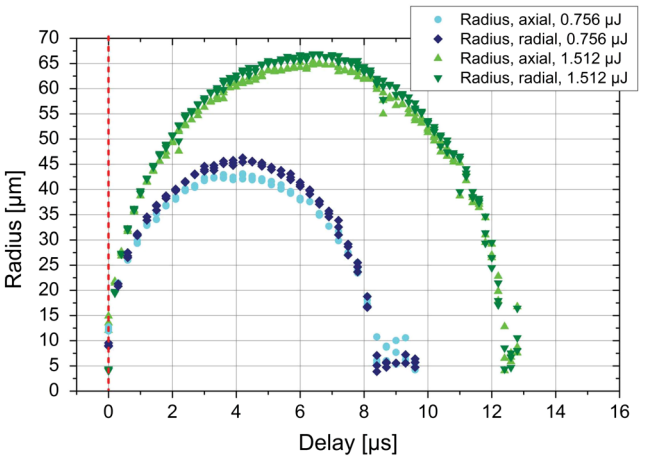

Fig. 2 Bubble radius (in radial and axial direction) over time for single laser pulses with energies of $E_{pulse} = 756$ nJ (6-times LIOB threshold) and $E_{pulse} = 1.512$ μJ (12-times threshold). The red dashed vertical line refers to an applied laser pulse.

objective), the measured single pulse energy breakdown threshold at the laser focal spot for the described experimental setup using the "μJewel" laser system is $E_{th} = 126 \pm 10$ nJ. The dedicated fluence at the laser focus is about 2.5 J/cm^2 under consideration of a diffraction-limited spot diameter (at given experimental parameters). Although no special care was taken to minimize spherical aberrations and the NA was below the limit of NA > 0.9, which ensures the absence of nonlinear effects in beam propagation,[12,17,31,32] the order of magnitude for the threshold is in good agreement with other findings in the literature (see overview in Ref. 31 and 14, 18, 30).

For a straight comparison with the following measurements of the temporal pulse-to-pulse interaction, the single bubble dynamics have been studied at different energies corresponding to the breakdown threshold. The results (bubble radius versus observation delay) for 6-times ($E_{pulse} = 756$ nJ) and 12-times ($E_{pulse} = 1.512$ μJ) the threshold can be seen in Fig. 2. Here, the bubble radius over delay is shown until coming up to the gas bubble phase (with radii of about 5 μm).

It is observable that there is a small difference between the bubble radii in axial as well as radial direction. After bubble formation, it shows an axial prolate deformation; the bubble is elongated along the laser optical axis and follows the plasma shape.[17] Afterwards, the shape changes to spherical where the energy state of the surface minimizes before getting oblate deformed due to the conservation of momentum.[33] Here, the entire effect is comparably weak due to the high focusing NA. Furthermore, it can clearly be recognized that the maximum radial bubble radius R_{max} (about 46 μm for $E_{pulse} = 756$ nJ and 66 μm for $E_{pulse} = 1.512$ μJ) and the oscillation period T_c (about 8.4 μs for $E_{pulse} = 756$ nJ and 12.4 μs for $E_{pulse} = 1.512$ μJ) increase as expected with increasing pulse energy (cf. Table 1). The bubble lifetimes deduced from these results correspond to a temporal interaction scenario (1) for $E_{pulse} = 756$ nJ pulse energy (temporal pulse overlap $\eta_t = 1.19$ with $\Delta t = 10$ μs) on the one hand and scenario (2) for $E_{pulse} = 1.512$ μJ (temporal pulse overlap $\eta_t = 0.81$ with $\Delta t = 10$ μs) on the other. Results of Student's t-test were considered significantly different at $p \leq 0.05$, whereas only distinct interaction scenarios were treated as independent samples. The comparison of the experimental-based maximum bubble radius R_{max} was not significantly different compared to the theoretical value $R'_{max}(T_c)$ (calculated from the measured bubble life time T_c by using the Rayleigh equation[12]) for both analyzed laser pulse energies ($t > 0.1133$, t-test).

3.2 *Dynamics of the Temporal Pulse-to-Pulse Interaction with Constant Repetition Rate of 100 kHz*

As compared to the single bubble dynamics, a series of equal laser pulses temporally separated by $\Delta t = 10$ μs results in very different bubble dynamics. Furthermore, since differences between the outcomes of the two experimental scenarios can be found, the results are presented for each interaction scenario or rather overlap parameter η_t.

3.2.1 *Interaction scenario of focusing a subsequent laser pulse after cavitation bubble collapse ($\eta_t > 1$)*

When focusing two laser pulses with an energy of each 756 nJ and an interval time of $\Delta t = 10$ μs, the cavitation bubble induced by the first pulse has a lifetime of about 8.7 μs [cf. Fig. 3(a)]. This means that the subsequent laser pulse impinges on the persistent gas bubbles, which are located at the focal spot after the collapse of the cavity. In this case, the temporal overlap parameter is $\eta_t = 1.15$. The dynamics of the cavitation bubble related to the second pulse are influenced by this, as can be seen in Figs. 3(a) and 4, evidenced by large statistical variation in radius. Whereas in principle, there is a similar radius course in the temporal development as in the already collapsed cavitation bubble, the reproducibility of the event decreases and hence the variation increases significantly. However, if the two laser pulses are focused at the same place with an interval of $\Delta t = 20$ μs, the temporal overlap parameter is about $\eta_t = 2.22$, the interaction picture changes so that for both laser pulses a LIOB and a cavitation bubble dynamic follow, which corresponds to the single-pulse dynamics [see Figs. 3(b) as well as 4]. This behavior is the same for an increased pulse energy of $E_{pulse} = 1.512$ μJ and a resulting overlap parameter of $\eta_t = 1.67$ [see Figs. 3(d) and 6]. Finally, a measurement was performed with three consecutive

Table 1 Overview of the comparison between the experimental results and theory for the single cavitation bubble dynamics with pulse energies of $E_{pulse} = 756$ nJ (6-times LIOB threshold) and $E_{pulse} = 1.512$ μJ (12-times threshold). The results of the t-test confirm the good compliance between experimental results and theory.

Pulse energy	Exp. value (R_{max})	Exp. value (T_c)	Theory value $R'_{max}(T_c)$	Difference ($\Delta R_{max} = R_{max} - R'_{max}$)	Result t-test (p-value)
756 nJ	45.71 ± 0.48 μm	8.4 μs	45.41 μm	0.30 μm	0.4408
1.512 μJ	66.17 ± 0.36 μm	12.4 μs	67.03 μm	–0.86 μm	0.1133

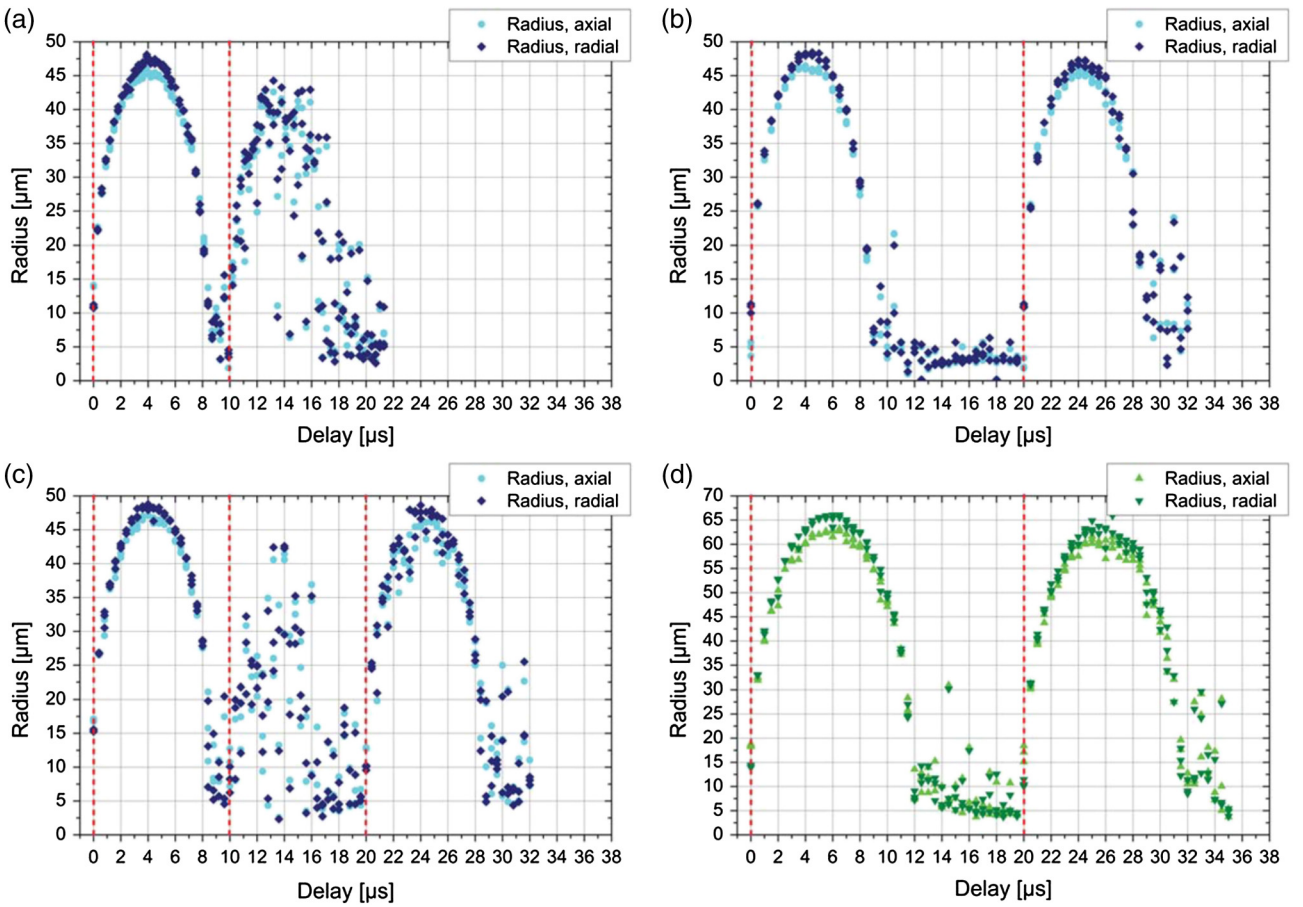

Fig. 3 Bubble radius over time delay for two laser pulses with $E_{pulse} = 756$ nJ and a temporal separation of (a) $\eta_t = 1.15$ ($\Delta t = 10$ μs) and (b) $\eta_t = 2.22$ ($\Delta t = 20$ μs). (c) Bubble radius over time for three laser pulses with $E_{pulse} = 756$ nJ and a temporal separation of $\eta_t = 1.09$ ($\Delta t = 10$ μs) for the first two pulses. (d) Bubble radius over time delay for two laser pulses with $E_{pulse} = 1.512$ μJ and a temporal separation of $\eta_t = 1.67$ ($\Delta t = 20$ μs). The red dashed vertical lines refer to an applied laser pulse.

laser pulses [cf. Fig. 3(c)]. There is a combination of the interaction images of the previous two series of measurements: Whereas the first pulse induces an optical breakdown, the second one encounters remaining gas bubbles at its focus (overlap parameter $\eta_t = 1.09$). This again results in a strong fluctuation of the second bubble's radius [compare to course in Fig. 3(a)]. In turn, the third laser pulse shows again an interaction dynamic that is more similar to that of a single pulse. However, it should be noted that the standard radius' variance compared to the first oscillation cycle slightly increases.

An explanation of the different observations described above is as follows. After the cavity collapse, the persistent gas bubbles have a statistical spatial distribution with respect to the laser focus. Generally, higher energetic cavitation bubbles can perform more than one oscillation cycle. This behavior would strongly influence the overlap and hence the interaction mechanisms of the subsequent laser pulses. Here, no significant further bubble expansion could be observed [cf. gas bubble phase in Figs. 3(b) and 3(d)]. A possible reason is the bubble deformation which results in a slightly asymmetric bubble collapse and prevents another sufficient compression of the focal volume. Due to the small time delay regarding the cavitation bubble collapse, these gas bubbles have a radius of up to 15 μm (cf. Fig. 4). This leads to a decrease in the reproducibility of the process, because in principle the subsequent pulse can encounter either a gas bubble or a water volume in between. Focusing the laser pulse into a gas bubble, there is possibly scattering, reflection or refraction of a certain ratio of incoming light at the surface; so that the quality of the laser focus, the laser pulse energy within the focus and, thus, the focal laser fluence may decrease. Here, with pulse energies well above the breakdown threshold the beam waist is supposably larger than the gas bubble radius. Hence, depending on the gas bubble dimensions as well as its position, the energy conversion will be influenced by the physical effects mentioned above. If the gas bubble is small compared to the laser focus, the conversion efficiency will be decreased in a negligible way: the second cavitation bubble will be similar to the first pulses'. With increasing bubble diameter and influence, the conversion efficiency and hence the resulting cavity diameter will decrease. Due to the variation of gas bubble properties, there are all possible intermediate cases with different bubble radii and temporal behavior. These different cases occur statistically, which results in an increasing deviation of radii analyzed by time-resolved photography (see different pictures for $\Delta t = 10$ μs at the same time delay at Fig. 4).

For pulse energies close to the breakdown threshold, the gas bubble diameter is in the range of the focus waist. In this case, it can be assumed additionally to the interaction mechanisms described in Sec. 3.2.2, that even the gas bubble completely

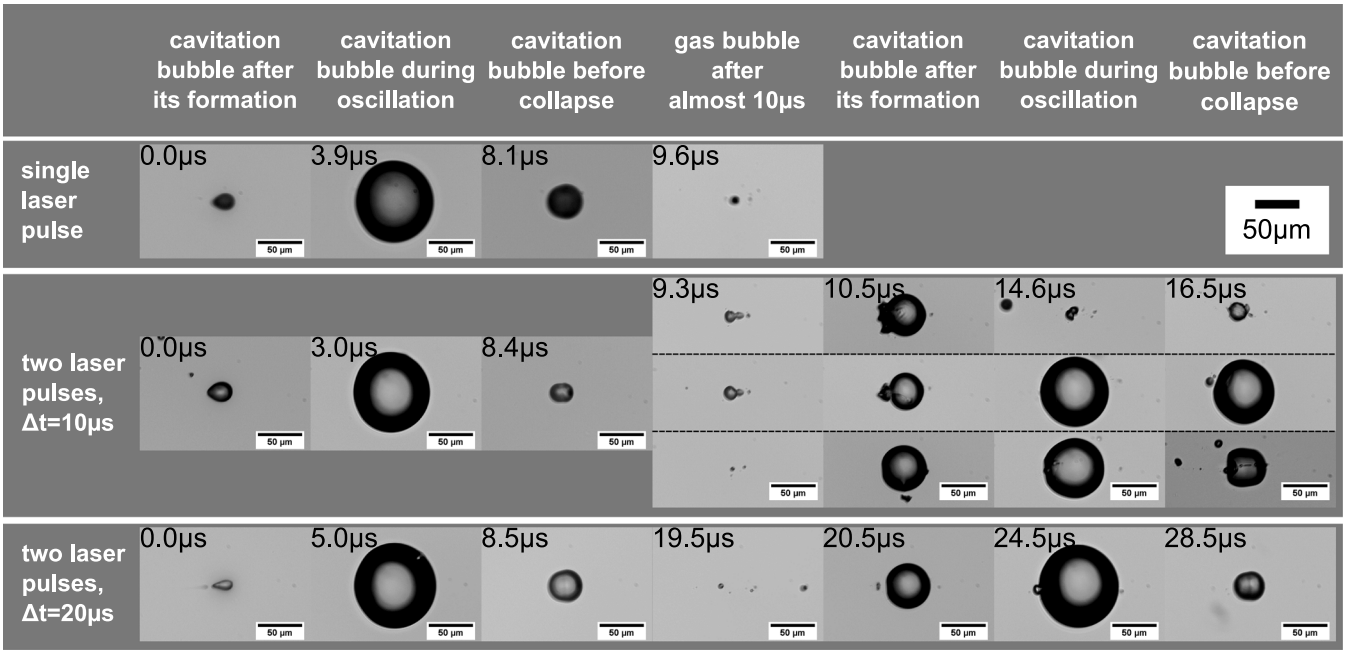

Fig. 4 Selected pictures of the cavitation bubbles created with a pulse energy of $E_{\text{pulse}} = 756$ nJ and different temporal separation. Each column shows pictures of cavitation bubbles within the same stage of oscillation, created by the first or the second laser pulse. For a pulse separation of $\Delta t = 10$ μs, the three different photos for the same delay reflect the variation of energy conversion and hence resulting cavitation bubble size. The scale bar signs 50 μm.

prevents a further LIOB. Within the vapor-filled bubble, the threshold for LIOB in the water vapor is significantly higher than in the surrounding liquid water.[34,35] Hence, if the subsequent pulse mainly hits vapor, both the focus distortions and the higher threshold impair the second optical breakdown process.

Further confirmation of this hypothesis derives from the other two measurements at the same laser pulse energy [cf. scenarios in Figs. 3(b) and 3(c)]. If the subsequent laser pulse has a larger time interval (here 20 μs) and thus temporal overlap parameter η_t, the probability to meet with a large diameter gas bubble of the first one at its focal point decreases for this second pulse (see gas bubble dimensions at 19.5 μs in Fig. 4). Therefore, another cavitation bubble of the unaffected size is formed in almost all cases; the variation of conversion efficiency decreases. In some of the picture, the small persistent gas bubbles can be observed as an unwanted side effect close to the surface of the second cavitation bubble (for example, at 10.5 μs for $\Delta t = 10$ μs in Fig. 4).

The application of three directly successive pulses [see Fig. 3(c)] leads to a mixed form of the previously described results. The dynamics after application of the second pulse again strongly differ from the typical course of bubble radius due to a single laser pulse. In turn, the third pulse leads to increased probability of a LIOB again, and hence, a cavitation bubble with nearly a single bubble's behavior appears. The slightly increased statistical variation of the third cavitation bubble radius results from an influence of the residual bubble due to the second laser pulse [cf. scenario shown in Fig. 3(a)]. Only in rare cases, the second pulse leads to a full-size cavitation bubble like the first pulse does. If so, there is a persistent gas bubble with similar dimensions as for an unaffected single pulse bubble oscillation. Hence, the conversion efficiency of the subsequent third laser pulse is slightly decreased. However, in most of the cases, the second cavitation bubble radius is decreased and, therefore, there will be no or insignificant small persistent bubbles after the second cavity's collapse. As for the scenario shown in Fig. 3(b), the influence on the third pulse is negligible. In conclusion, the superposition of these cases results in the observable radius course for the third pulse with an increased variance. Unfortunately, conditional probabilities between consecutive pulses cannot be displayed by the time-resolved photography method, which is based on a strict reproducibility of events.

Overall, the findings within the interaction scenario presented here are in very good agreement with the experimental results and increasing statistical variations as shown for ns-laser pulses in Ref. 23.

3.2.2 *Interaction scenario of focusing a subsequent laser pulse into existing cavitation bubble ($\eta_t < 1$)*

By changing the laser pulse energy to $E_{\text{pulse}} = 1.512$ μJ, corresponding to approximately 12 times the breakdown threshold, the other interaction scenario occurs: after a temporal pulse interval of $\Delta t = 10$ μs, the subsequent pulse impinges on the cavitation bubble of the previous pulse, currently going through the collapse phase of its oscillation cycle (cf. Fig. 6). In Fig. 5(a), the radius evaluation of this interaction mechanism is depicted, here $\eta_t = 0.82$. Compared to the previously studied scenario, it is noticeable that the second pulse neither seems to have an influence on the running oscillation, nor effects rising from a second cavitation bubble. In fact, the images as well as the measured bubble radius over time do not show evidence of the application of a second laser pulse (see cavitation bubble after 10 μs in Fig. 6).

Again, three directly successive laser pulses were focused at a distance of 10 μs ($\eta_t = 0.83$) at the same position [see

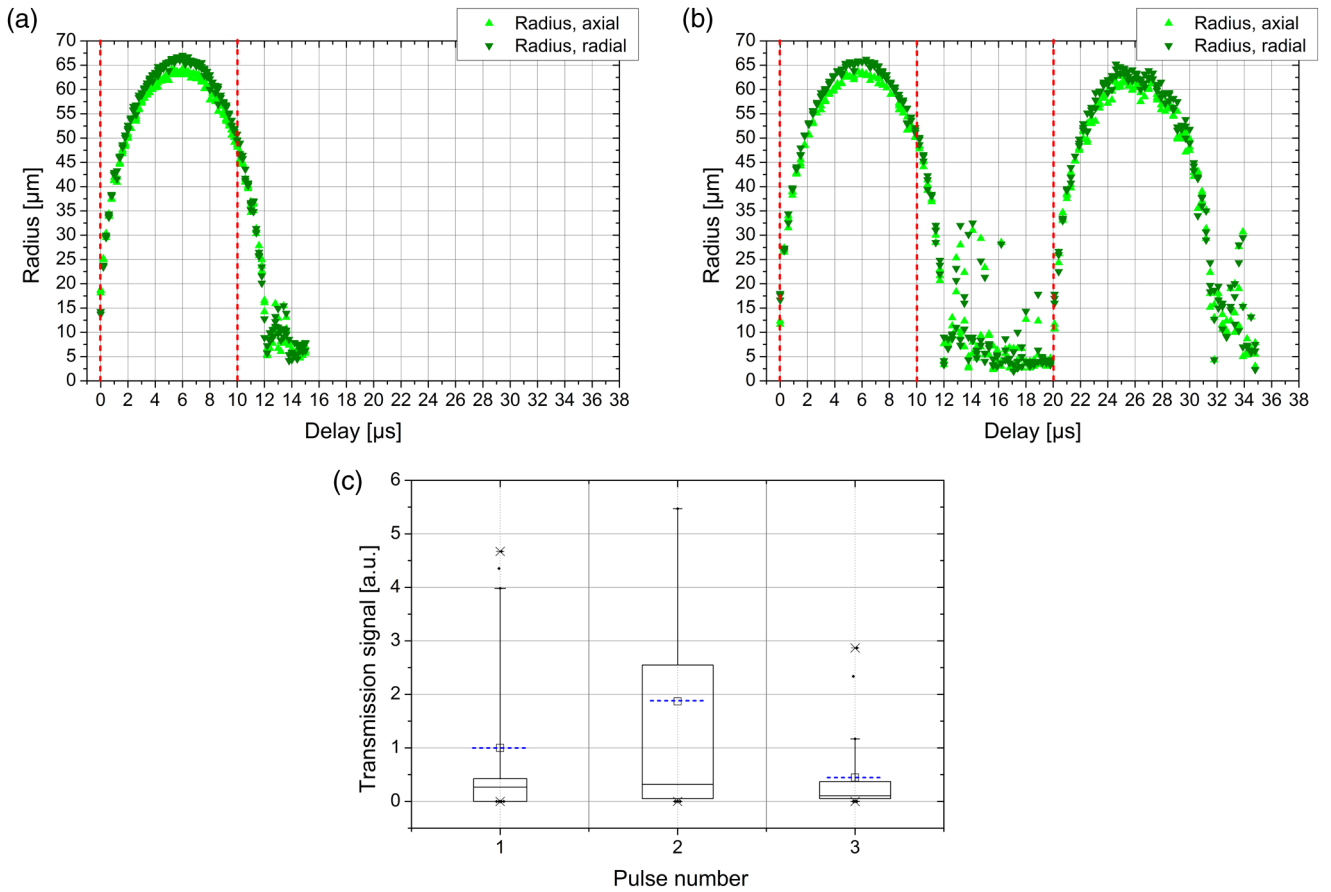

Fig. 5 Bubble radius over time for two laser pulses with $E_{\text{pulse}} = 1.512\ \mu\text{J}$ and a temporal separation of (a) $\eta_t = 0.82$ ($\Delta t = 10\ \mu\text{s}$) (including radius of first gas bubbles). (b) Bubble radius over time delay and (c) photodiode signal over pulse number for three laser pulses with $E_{\text{pulse}} = 1.512\ \mu\text{J}$ and a temporal separation of $\eta_t = 0.83$ ($\Delta t = 10\ \mu\text{s}$) for the first two pulses. The red dashed vertical lines refer to an applied laser pulse. The mean transmission value is marked with a blue dashed horizontal line.

Fig. 5(b)]. In turn, the result corresponds to a superposition of the two preceding results. It reveals the same interaction picture as the previous measurement, which means that the first and third laser pulses result in a LIOB and cavitation bubble dynamics similar to that of a single laser pulse. However, the second pulse, which is focused into the existing cavity, has no detectable effect on the medium. A laser power measurement behind the cuvette performed in this scenario reveals an increased central transmission for this second of the three pulses [see Fig. 5(c)]. In the associated graph, the signal of the photodiode is depicted for 24 measurements. Due to the exact signal interval of $\Delta t = 10\ \mu\text{s}$ an unambiguous assignment to the laser pulses was possible. Here, the signal is shown in arbitrary units and normalized to the mean value of the first pulse's transmission. It reveals that the mean value (horizontal blue dashed line) of the second pulse has a central transmission up to twice as large as those of pulses resulting in a LIOB [see Pulses 1 and 3 in Fig. 5(c)].

The observations can be explained as follows: due to the refractive index change at the cavity surface, a minimal focus shift (whose magnitude depends intricately on parameters such as bubble deformation, phase of the oscillation cycle, focusing NA, etc.) along the laser optical axis is conceivable. Nevertheless, if the focus is still located within the cavity, it encounters this cavitation bubble filled with low-density water vapor.[23] Water vapor, unlike liquid water, can no longer be assumed to be an amorphous semiconductor,[16] so that the ionization energy increases dramatically.[23] The increase in the threshold energy required for LIOB inside a cavitation bubble is appreciated to up to six orders of magnitude due to the gas phase inside.[34,35] Therefore, the laser pulse energy is not sufficient to induce another optical breakdown; it should be noted that the occurrence of nonlinear absorption effects still cannot be excluded. The determined ratio of about 2 between the transmission signal measured for the second and first pulses can be compared to the transmission values in case of a LIOB in the literature.[17,30] The transmission of a 300 fs-laser pulse with a wavelength of 580 nm at 10 times the breakdown threshold equates to 54 to 61% due to an occurring optical breakdown.[17,30] Hence, the transmission of the subsequent laser pulse which impinges the cavitation bubble should yield a 1.63- to 1.85-times higher value, if it has a transmission of 100%. Thus, the findings of the presented study are in good agreement with the literature.[17,30] However, it has to be mentioned that the Ref. 30 does not take into account the focusing angle as well as that the detector position differs from the one in the presented study. The mean value of the central transmission of the third pulse, being decreased compared to the first one, might be traced to a rise in scattering structures like gas bubbles in the course of the pulse sequence.

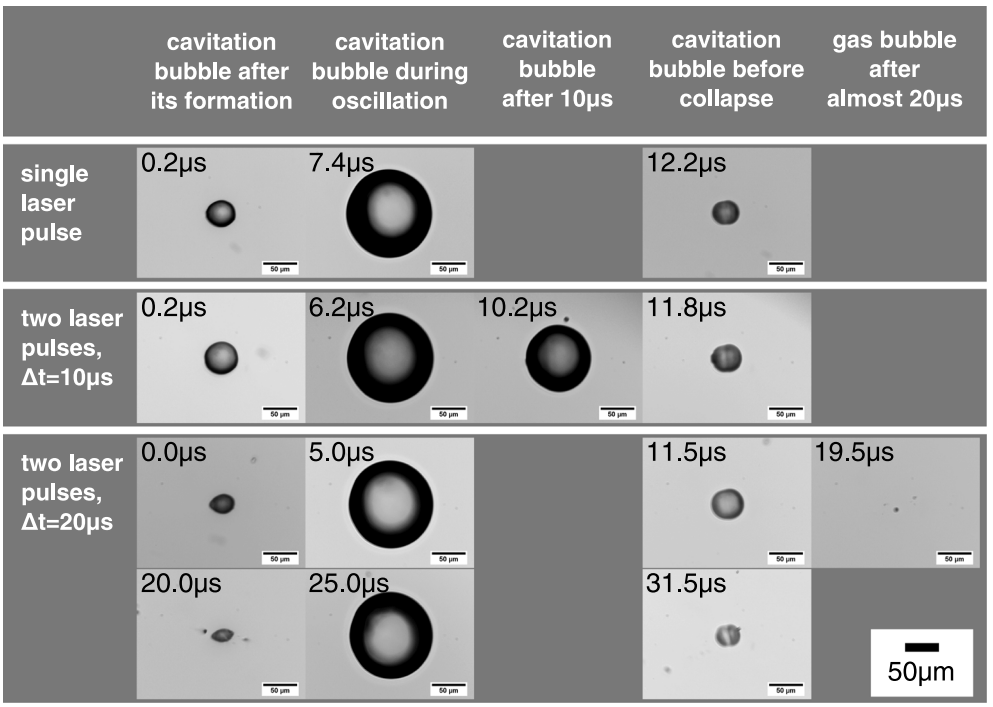

Fig. 6 Selected pictures of the cavitation bubbles created with a pulse energy of $E_{\text{pulse}} = 1.512\ \mu$J and different temporal separation. Each column includes pictures of cavitation bubbles within the same stage of oscillation, created by the first or the second laser pulse. For a pulse separation of $\Delta t = 10\ \mu$s, the cavitation bubble after 10 μs and hence almost after the second laser pulse arrived is shown with no visible influence. The scale bar signs 50 μm.

This interaction picture is further supported by the other measurements with the same pulse energy [belonging to Fig. 3(d)]. In a temporal pulse interval of 20 μs ($\eta_t = 1.67$), the first interaction process is finished upon arrival of the next laser pulse, so that the focus spot has almost completely regenerated (cf. explanation in Ref. 23). For the small residual probability of still existing gas bubbles there are small statistical fluctuations in conversion efficiency and radius as evidence. Observing the interaction of three consecutive pulses, almost no difference to the previous series of measurement can be seen. This confirms the assumption that the second laser pulse interacts with the medium in a negligible way.[23] Even if there are nonlinear absorption processes at the point of focus, the transmission measurement shows that the central absorption within the focal volume is significantly lower than for the first and third pulses. Thus, a pulse is applied to the sample, whose interaction effect cannot be used mechanically.[23] In fact, an increased transmission in a medical treatment of the anterior

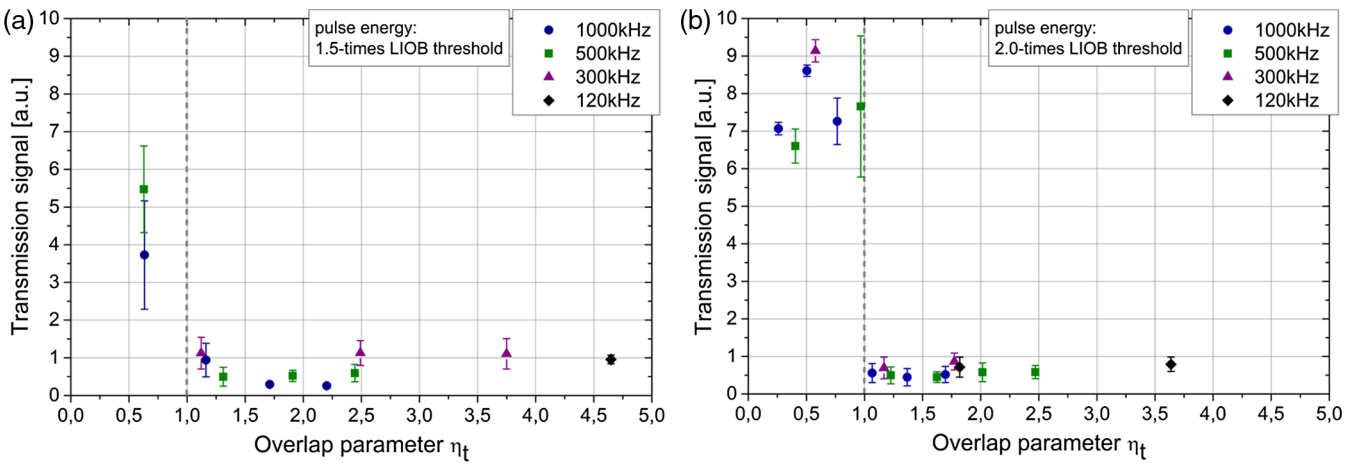

Fig. 7 Photodiode signal of a subsequent laser pulse against the overlap parameter η_t for various laser repetition rates: 1000, 500, 300, and 120 kHz of the "Cazadero" laser system. The laser pulse energy is in accordance with (a) 1.5-times the breakdown threshold and (b) 2.0-times the breakdown threshold. In both cases, the signal is increased for a temporal pulse overlap ($\eta_t < 1$) and nearly constant for $\eta_t > 1$.

eye would influence the retina most. Here, mainly linear absorption of the laser energy takes place, so that an increase of transmission could lead to a thermal damage in the worst case.

3.3 *Laser Transmission in Both Interaction Scenarios for Different Laser Repetition Rates*

Additionally, these experiments for analyzing the two interaction scenarios using a constant laser repetition rate were supplemented by a variation of the temporal pulse separation. Here, the series of measurement was repeated with the "Cazadero" laser system and its different repetition rates for various laser pulse energies. In this way, many different values for the temporal overlap η_t could be achieved.

In Fig. 7, the photodiode signal is shown versus the overlap parameter for two different pulse energies corresponding to the LIOB threshold. Again, the central transmission is depicted in arbitrary units and normalized to the mean value of the first pulse's photodiode signal. It can clearly be seen that the results show a good agreement with the former ones (cf. Sec. 3.2.2). In both interaction scenarios and for all repetition rates, the photodiode signal depends on the pulse overlap in the same way. On the one hand, a temporal pulse overlap ($\eta_t < 1$) of subsequent laser pulses leads to a suppression of a second laser-induced optical breakdown. There is no second cavitation bubble observable in the time-resolved imaging and the laser photodiode signal behind the laser focus clearly increases. However, in this case, the quantitative comparison of the signal increase with the literature[17,30] is hardly possible. A probable reason is the increasing influence of the focusing angle on the energy transmission for decreasing applied pulse energies.[17] Furthermore, due to the restricted central detector positioning, no quantitative results for the increase of energy transmission of the subsequent laser pulse could be obtained. On the other hand, if the laser pulse impinges on the focal volume after collapse of the previous cavitation bubble, the photodiode signal decreases as well. While the statistical variability of the photodiode signal rises for values of $\eta_t \approx 1$, the signal converges to a minimum value for decreasing overlap (increasing η_t).

The observation of a higher statistical variability is based on the deviation of cavitation bubble collapse: at $\eta_t = 1$ a relatively sharp transition between the two interaction scenarios is located. Depending on whether the collapse is completed or not, the subsequent pulse impinges on the cavitation bubble or on a vapor bubble or rather water. Due to the experimental reproducibility, which is high for water as a sample medium but not 100%, the detailed effects may differ for the same laser parameters in this transition zone. The photodiode signal stagnation can be explained as follows: with the increasing overlap parameter there is an approach to the interaction of single laser pulses with the medium. The larger the time separation of two subsequent pulses or rather the overlap parameter, the larger the progression in the process of regeneration of the focal volume. This means that the probability of impinging on remaining gas bubbles decreases for the following pulse.

Furthermore, it could be shown that the oscillation of the cavitation bubble due to the first focused laser pulse is not influenced by the following second pulse at all. In the time-resolved pictures of the cavitation bubble, no interaction effect such as a deformation of the bubble surface can be observed. In addition, analyzing the bubble radius over time for a single cavitation bubble and for a cavity hit by a subsequent laser pulse at different stages of oscillation shows no changes of the cavitation bubble lifetime T_c or the maximum bubble radius R_{max}. The bubble lifetime versus the applied laser pulses is shown in Fig. 8. Results of Student's t-test were considered significantly different at $p \leq 0.05$, whereas only distinct interaction scenarios were treated as independent samples. The bubble oscillation time T_c of the cavitation bubble created by the first applied laser pulse was not significantly different compared to the unaffected single bubble oscillation time ($t > 0.068$, t-test). Again, this supports the assumption that the second laser pulse interacts with the medium in a negligible way. Thus, the following pulse is focused to the sample without having a stake in the mechanical cutting effect.

3.4 *Interaction of Subsequent Laser Pulses in Gelatin as Sample Medium*

For the sake of simplicity, water has been used as a sample medium for the first experiments. Although water is acceptable as a first sample medium for biological tissue, the rheological properties between water as a liquid and tissue as an aqueous more solid medium differ strongly. For that reason, the basic experiments of the interaction process within the two scenarios were also performed in different concentrations of porcine gelatin (1%, 2%, and 5%). While the 1% gelatin-water solution is still kind of colloidal, the 5% composition is almost an aqueous solid. To generate the two interaction scenarios introduced above, the following energy ratios compared to the breakdown threshold in water were chosen: (1) $\eta_t > 1$: 3.7-times and (2) $\eta_t < 1$: 8.4-times LIOB threshold. The energy and threshold measurements were performed in water because for this sample medium an influence due to a local damage by a previous pulse can be excluded. Furthermore, the LIOB threshold in gelatin like in polyacrylamide (PAA) as well as agar gel[36–39] is nearly the same as in water. Here again, the energy was varied to scale the bubble lifetime and hence the temporal overlap with the subsequent laser pulse. The results of the generated cavitation bubble radius versus time can be seen in Fig. 9.

In any case, the results show that the findings for water as sample medium are completely transferable to gelatin. It is

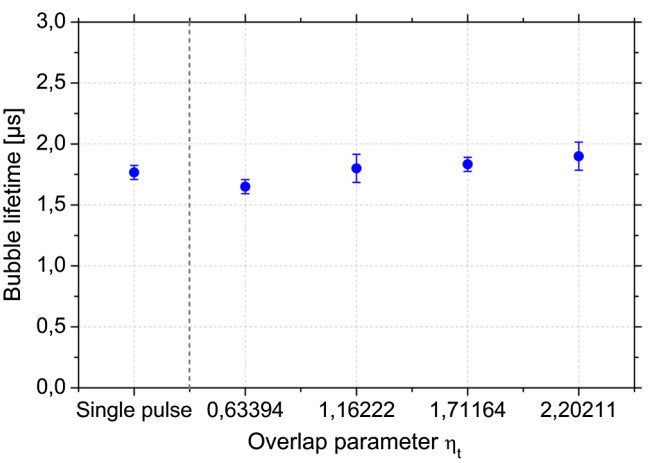

Fig. 8 Cavitation bubble lifetime T_c versus the applied laser pulses for a repetition rate of 1000 kHz. A single laser pulse and two laser pulses with various overlap parameter η_t were focused and the oscillation time of the first pulse's cavitation bubble was analyzed; no difference between the examined interaction scenarios can be observed.

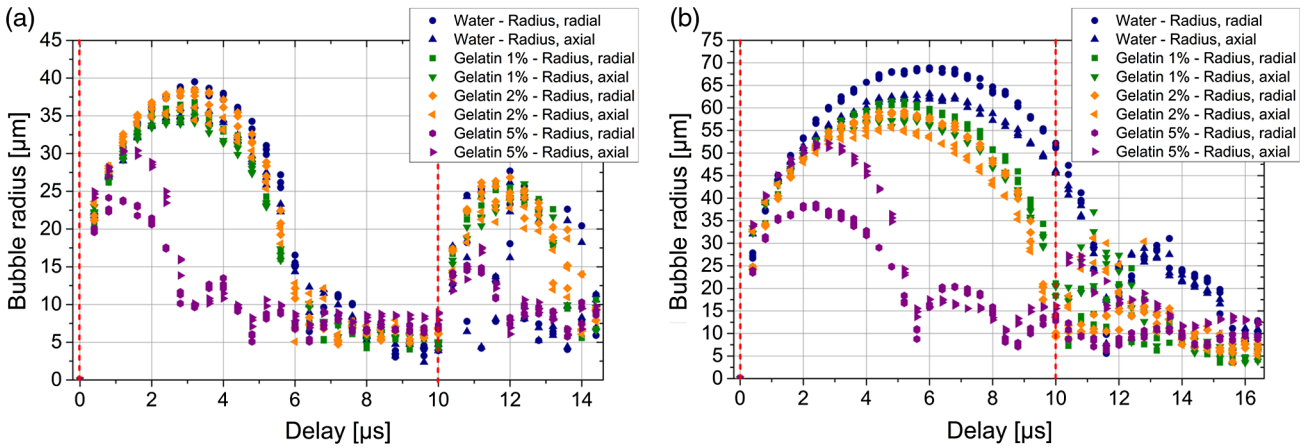

Fig. 9 Bubble radius over time for two laser pulses with energies of (a) 3.7-times ($\eta_t > 1$ for water) and (b) 8.4-times ($\eta_t < 1$ for water) the breakdown threshold in water. The course of radius is shown for water and gelatin of different concentrations (1%, 2%, and 5%) as sample medium. The red dashed vertical lines refer to an applied laser pulse.

observable that the maximum bubble radius at the same applied laser pulse energy decreases, but the dependency of the interaction mechanisms on the overlap parameter persists. In detail, for $\eta_t > 1$, there is a second cavitation bubble generation after the gas bubble phase due to the application of a further laser pulse after 10 μs. Even if the second cavity is smaller compared to the first one, its maximum radius scales with the initial maximum bubble radius. Additionally, this value depends on the gelatin concentration: with increasing gelatin percentage and hence rigidity the maximum bubble radius and the bubble lifetime decrease; this behavior was described in other publications before.[36–38] An exception can be observed for the 1% and 2% gelatin solution in Fig. 9(a). Here, the higher concentration results in a slightly increased maximum bubble radius R_{max} as well as life time T_c. A possible reason can be found within the experimental procedure: On the one hand, the positioning of the cuvette during sample exchange is not perfectly reproducible which leads to minimal differences in the breakdown threshold. On the other hand, small inaccuracies in the gelatin concentration affect the resulting cavitation bubble. Overall, for lower pulse energies (here 3.7-times breakdown threshold in water), the variation of bubble dimensions for different gelatin solutions is expected to be much smaller than for an increasing deposited laser energy [cf. Fig. 9(b)]. While the quantitative progress of the radius with an atypical small second bubble's oscillation radius cannot be explained here, the qualitative results match well with the measurements in water shown before.

For the second series of measurement, the subsequent laser pulse impinges the cavitation bubble to water; for the 1% as well as 2% gelatin, the second laser pulse is close to the collapse time of the first pulse's cavity. For 5% gelatin, the bubble collapse appeared some microseconds before; further oscillation cycles can be observed afterwards. Overall, this means that the effective temporal overlap parameter depends on the medium at constant pulse energy. For $\eta_t > 1$ (water), no further cavitation bubble occurs as a result of the second focused laser pulse. At $\eta_t \approx 1$ (1% and 2% gelatin), there is a cavitation bubble oscillation after application of the second laser pulse but a clear distinction between this laser pulse and a second oscillation cycle of the first bubble based on the resulting bubble radius is not possible. Only for $\eta_t < 1$ and 5% gelatin, there is a significant increase of bubble radius at a delay of 10 μs; a new cavity is created by the subsequent laser pulse.

These results in porcine gelatin show that the previous experimental results for water as a sample medium can be transferred to mechanically more rigid aqueous media like gelatin or even isotropic biological tissue like vitreous body. Due to the decrease of maximum bubble radius with increasing concentration, only the laser pulse energies have to be increased to achieve the same temporal overlap of subsequent laser pulses.

4 Conclusion and Outlook

We presented an analysis of the cavitation bubble dynamics of temporally separated fs-laser pulses using time-resolved photography. It is a systematic investigation in which the behavior of temporal pulse-to-pulse interaction was studied regarding the dissection quality of future generation ophthalmic laser systems.

In a previous publication, we could show the influence of temporal separated pulses and hence cavitation bubbles on the dissection efficiency and quality during laser surgery.[29] Here, the temporal overlap of pulses and bubbles leads to a reduced effectiveness in terms of the used fluence for the cutting process. The energy of laser pulses impinging persistent gas bubbles due to the previous pulse (overlap parameter $\eta_t > 1$) will be partly lost for the cutting process itself. In contrast, for applying subsequent laser pulses on still oscillating cavitation bubbles ($\eta_t < 1$), a complete loss of the laser pulse energy for the cutting process occurs, which may contribute to a higher level of unwanted side effects in the surrounding tissue.[23] An increased laser energy transmission would mean a linear thermal influence on the retina which might induce damage. Undoubtedly, this should be avoided by adjusting parameters in order to ensure a minimally invasive procedure and at the same time increase its efficiency. Based on these results, further experiments could additionally lead to a better understanding of the transferability between water and more anisotropic biological tissue, such as crystalline lens or cornea.

In ophthalmic laser surgery, pulse energies close or slightly above the breakdown threshold are applied to dissect the tissue. In water, such fs-laser-induced cavities have radii in the range of up to some micrometers and lifetimes of some microseconds. This means that a repetition rate of some 100 kHz would

lead to an overlap of a following pulse with the previous cavitation bubble. Focusing into the cavitation bubble itself will be additionally avoided by scanning the laser within the tissue. Therefore, the critical laser parameters depend on the repetition rate as well as on the scanning velocity.

While the presented results have elucidated the phenomena occurring during purely temporally varying cavitation-pulse overlap, the even more relevant scenario also includes a transverse spatial separation between consecutive pulses as it is the case in the scanning surgical laser procedure. With various transversal focal distances but without temporal separation, this was presented in a former publication[29] showing interesting phenomena, such as the build-up of jets. A thorough coverage of more complex combinations of spatial and temporal pulse-to-pulse separations is part of further experimental studies. They will be the topic of an upcoming publication where an exact comparison with the medical laser application is possible. Thus, final consecutions to the cutting process of high-repetition rate fs-laser systems will be conducted.

Acknowledgments

Nadine Tinne acknowledged support from the fellowship "Foundation of German Business," Berlin, Germany (funded by Germany's Federal Ministry for Education and Research). This work was funded by the German Research Foundation (DFG); DFG-Grant No. Ri 2066/2-1.

References

1. P. S. Binder, "One thousand consecutive intralase laser in situ keratomileusis flaps," *J. Cataract Refract. Surg.* **32**(6), 962–969 (2006).
2. T. Juhasz et al., "Corneal refractive surgery with femtosecond lasers," *IEEE J. Quantum Electron.* **5**(4), 902–910 (1999).
3. G. M. Kerzirian and K. G. Stonecipher, "Comparison of the IntraLase femtosecond laser and mechanical keratomes for laser in situ keratomileusis," *J. Cataract Refract. Surg.* **30**(4), 804–811 (2004).
4. H. Lubatschowski et al., "Application of ultrashort laser pulses for intrastromal refractive surgery," *Graef. Arch. Clin. Exp.* **238**(1), 33–39 (2000).
5. I. Ratkay-Traub et al., "First clinical results with the femtosecond neodynium-glass laser in refractive surgery," *J. Refract. Surg.* **19**(2), 94–99 (2003).
6. V. Nuzzo et al., "In situ monitoring of second harmonic generation in human corneas to compensate for femtosecond laser pulse attenuation in keratoplasty," *J. Biomed. Opt.* **12**(6), 064032 (2007).
7. M. P. Holzer et al., "Intrastromal femtosecond laser presbyopia correction: 1-year results of a multicenter study," *J. Refract. Surg.* **28**(3): 182–188 (2012).
8. Z. Nagy et al., "Initial clinical evaluation of an intraocular femtosecond laser in cataract surgery," *J. Refract. Surg.* **25**(12), 1053–1060 (2009).
9. T. Ripken et al., "Fs-laser induced elasticity changes to improve presbyopic lens accommodation," *Graef. Arch. Clin. Exp.* **246**(6), 897–906 (2008).
10. H. Lubatschowski, "Overview of commercially available femtosecond lasers in refractive surgery," *J. Refract. Surg.* **24**(1), 102–107 (2008).
11. M. C. Knorz and U. Vossmerbaeumer, "Comparison of flap adhesion strength using the amadeus Microkeratome and the intralase iFS femtosecond laser in rabbits," *J. Refract. Surg.* **24**(9), 875–878 (2008).
12. A. Vogel et al., "Mechanisms of femtosecond laser nanosurgery of cells and tissues," *Appl. Phys. B* **81**(8), 1015–1047 (2005).
13. P. K. Kennedy, "A first-order model for computation of laser-induced breakdown thresholds in ocular and aqueous media: Part I-theory," *IEEE J. Quant. Electr.* **31**(12), 2241–2249 (1995).
14. P. K. Kennedy et al., "A first-order model for computation of laser-induced breakdown thresholds in ocular and aqueous media: Part II-comparison to experiment," *IEEE J. Quant. Electr.* **31**(12), 2250–2257 (1995).
15. P. K. Kennedy, D. X. Hammer, and B. A. Rockwell, "Laser-induced breakdown in aqueous media," *Prog. Quantum Electron.* **21**(3), 155–248 (1997).
16. C. A. Sacchi, "Laser-induced electric breakdown in water," *J. Opt. Soc. Am. B* **8**(2), 337–345 (1991).
17. A. Vogel et al., "Energy balance of optical breakdown in water at nanosecond to femtosecond time scales," *Appl. Phys. B* **68**(2), 271–280 (1999).
18. J. Noack et al., "Influence of pulse duration on mechanical effects after laser-induced breakdown in water," *J. Appl. Phys.* **83**(12), 7488–7495 (1998).
19. D. X. Hammer et al., "Experimental investigation of ultrashort pulse laser induced breakdown thresholds in aqueous media," *IEEE J. Quant. Electr.* **32**(4), 670–678 (1996).
20. C. B. Schaffer, "Interaction of femtosecond laser pulses with transparent materials," Ph.D. Thesis, Harvard Univ. (2001).
21. A. Vogel, "Optical breakdown in water and ocular media, and its use for intraocular photodisruption," Habilitation Dissertation, Medical Univ. of Lübeck (1998).
22. S. B. Kiselev, "Kinetic boundary of metastable states in superheated and stretched liquids," *Phys. A* **269**, 252–268 (1999).
23. K. Jungnickel and A. Vogel, "Efficiency of bursts in intraocular Nd: YAG laser surgery," *Lasers Light Ophthalmol.* **5**(2), 95–99 (1992).
24. T. Juhasz et al., "Time-resolved observations of shock waves and cavitation bubbles generated by femtosecond laser pulses in corneal tissue and water," *Lasers Surg. Med.* **19**(1), 23–31 (1996).
25. E. N. Glezer et al., "Minimally disruptive laser-induced breakdown in water," *Opt. Lett.* **22**(23), (1997).
26. A. Köhler, "Gedanken zu einem neuen Beleuchtungsverfahren für mikrophotographische Zwecke," Zeitschrift für wissenschaftl. Mikroskopie X, 433–440 (1893).
27. W. Lauterborn and W. Hentschel, "Cavitation bubble dynamics studied by high speed photography and holography: Part 1," *Ultrasonics* **23**(6), 260–268 (1985).
28. N. Tinne et al., "Impact of a temporal pulse overlap on laser-tissue-interaction of modern ophthalmic laser systems," *Proc. SPIE* **8579**, 857903 (2013).
29. N. Tinne et al., "Interaction dynamics of spatially separated cavitation bubbles in water," *J. Biomed. Opt.* **15**(6), 068003 (2010).
30. D. X. Hammer et al., "Shielding properties of laser-induced breakdown in water for pulse durations from 5 ns to 125 fs," *Appl. Opt.* **36**(22), 5630–5640 (1997).
31. A. Vogel et al., "Femtosecond-laser induced nanocavitation in water: implications for optical breakdown threshold and cell surgery," *Phys. Rev. Lett.* **100**(3), 038102 (2008).
32. C. L. Arnold et al., "Computational model for nonlinear plasma formation in high NA micromachining of transparent materials and biological cells," *Opt. Express* **15**(16), 10303–10317 (2007).
33. I. Akhatov et al., "Collapse and rebound of a laser-induced cavitation bubble," *Phys. Fluids* **13**(10), 2805–2819 (2001).
34. Y.-L. Chen, J. W. L. Lewis, and C. Parigger, "Probability distribution of laser-induced breakdown and ignition of ammonia," *J. Quant. Spect. Rad. Trans.* **66**(1), 41–53 (2000).
35. Y.-L. Chen, J. W. L. Lewis, and C. Parigger, "Spatial and temporal profiles of pulsed laser-induced air plasma emissions," *J. Quant. Spect. Rad. Trans.* **67**(2), 91–103 (2000).
36. R. Evans et al., "Pump-probe imaging of nanosecond laser-induced bubbles in agar gel," *Opt. Express* **16**(10), 7481–7492 (2008).
37. E.-A. Brujan and A. Vogel, "Stress wave emission and cavitation bubble dynamics by nanosecond optical breakdown in a tissue phantom," *J. Fluid Mech.* **558**, 281–308 (2006).
38. F. Pérez-Gutierrez et al., "Time-resolved study of laser-induced bubbles and shockwaves in agar gel tissue phantoms," in *Proc. ASME 2008 Summer Bioengineering Conference* 193061, pp. 613–614 (2008).
39. F. Pérez-Gutierrez et al., "Short and ultrashort laser pulse induced bubbles on transparent and scattering tissue models," *Proc. SPIE* **6435**, 64350V (2007).

Nadine Tinne is a PhD student at the Laser Zentrum Hannover e.V, Germany. She received her diploma degree in physics from the Gottfried Wilhelm Leibniz University of Hannover, Germany, in 2009. Her current research interests include cavitation bubble phenomena and the interaction of subsequent disruption effects regarding the dissection quality in ophthalmic laser surgery. She is a student member of SPIE.

Biographies of the other authors are not available.